

A study on mechanical properties of 1H-type crystalline nickel ditelluride

Nguyen Danh Truong^{1,*}, Nguyen Van Quynh^{1,2}

¹*School of Mechanical Engineering, Hanoi University of Science and Technology,
1 Dai Co Viet, Hai Ba Trung, Ha Noi, Viet Nam*

²*Thanh Do University, km 15, Highway 32, Kim Chung, Hoai Duc, Ha Noi, Viet Nam*

*Email: truong.nguyendanh@hust.edu.vn

Received: 31 October 2022; Accepted for publication: 16 August 2023

Abstract. We used the molecular dynamic finite element method with Stillinger-Weber potential to study the mechanical behavior of monolayer 1H-type nickel ditelluride (1H-NiTe₂) sheets under uniaxial tension. As the size of the pristine 1H-NiTe₂ sheet increases, the Young's modulus in the armchair direction increases by 6.2 %, while that in the zigzag one decreases by 6.0 %. Both tend to be size-independent in larger sheets and approach the same value at around 54 N/m. The ultimate stress in the armchair direction remains almost unchanged but that in the zigzag one reduces by about 9.5 % as the size inclines. Besides the influence of size, our results show that single vacancy defects strongly affect the ultimate stress and strain while having no effect on Young's modulus and Poisson's ratio. When a Te atom is missing at the sheet's center, the ultimate stress in the armchair direction is reduced by 11.7 %, while a decrease of 16.0 % is caused by a Ni atom vacancy.

Keywords: Nickel ditelluride, mechanical properties, missing-atom defect, size effect, molecular dynamic finite element method.

Classification numbers: 5.4.5, 5.4.6.

1. INTRODUCTION

In recent times, nanomaterials have been of great interest to scientists because of their interesting properties in mechanics, electricity, and optics. Graphene and its nanomaterials were the first studied materials which are broadly employed in a range of applications from mechanics to electronics and from agriculture to biomedical science. Utilized as a semiconductor, a material has a requisite bandgap, but graphene does not [1 - 4], making it an exception. In contrast to graphene, transition metal dichalcogenides (TMDs) have been found to exhibit a finite bandgap with 1-2 eV [5] while maintaining the other appealing characteristics of nanomaterials.

Monolayer 1H-type crystalline nickel ditelluride (1H-NiTe₂) sheet is one of the TMDs synthesized by heating an ampoule containing the reaction mixture to 1000 °C [6], consisting a

Ni atom layer between two Te atom layers (see Figure 1). Unlike graphene, not much research has been conducted on 1H-NiTe₂ sheets. The NiTe₂ monolayer showed a strong thickness-tunable electrical property, with excellent conductivity and extraordinary breakdown current density [7]. The application capability of NiTe₂ in catalysis and nanoelectronics has been reported in [8]. Using molecular dynamics (MD) simulations, Jiang *et al.* discovered mechanical properties of 1H-NiTe₂ sheet in the dimension of 100 × 100 Å. They found out the two-dimension (2D) Young's modulus of the sheet to be 53.6 N/m and 53.2 N/m along the zigzag (ZZ) and armchair (AM) directions, respectively, and a Poisson's ratio of 0.32 along both directions [9]. Md. Faiyaz Jamil *et al.* also used MD simulation to investigate both 1T and 1H structures of NiTe₂[10]. They reported that the NiTe₂ layered atomic structure was regulated by brittle type failure. Increasing temperature and defect density minimized the ultimate stress and strain of NiTe₂. The ab initio calculations predicted a Young's modulus of 44 N/m and a Poisson's ratio of 0.14 for the 1T-NiTe₂ single layer [11].

To the best of the authors' knowledge, no work has studied the influence of size on mechanical behaviors of 1H-NiTe₂ sheets using the finite element method. The influence of defects on the mechanical properties of 1H-NiTe₂ sheets has not been investigated. Therefore, a more complete understanding of the mechanical properties of 1H-NiTe₂ nanosheets is needed before their great potential applications can be realized. The main goal of this work is to study the mechanical properties of 1H-NiTe₂ nanosheets. We simulated simple tensile tests by using the molecular dynamic finite element method (MDFEM) with Stillinger-Weber (SW) potential. Besides, the influence of size and vacancy defects on Young's moduli, Poisson's ratio, ultimate stress, and ultimate strain of the 1H-NiTe₂ nanosheets were estimated and discussed.

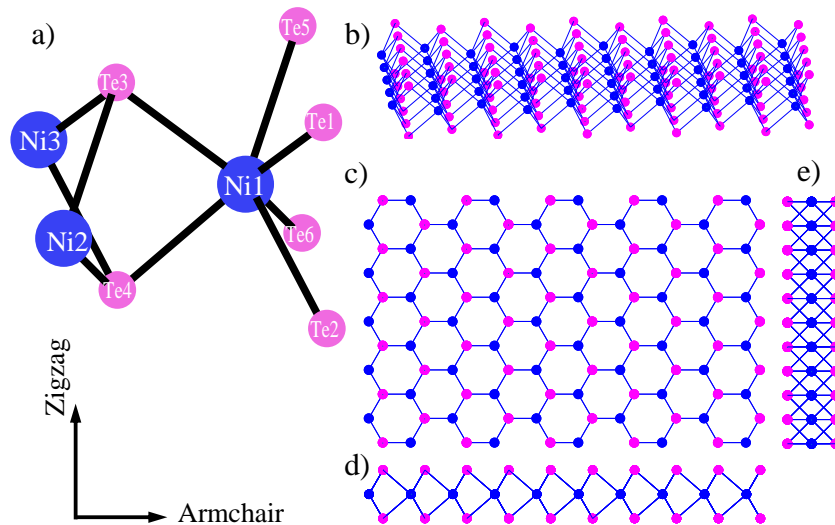


Figure 1. Configuration of the 1H-NiTe₂: a) Enlarged view of the nine nearest atoms; b) Three-dimension view; c) top view; d) front view; e) side view.

2. MODEL AND METHOD

Figure 1 depicts the atomic structure of 1H-NiTe₂ where six Te atoms are divided into upper and lower groups surrounding one Ni atom. The bond length between adjacent Ni and Te atoms is 2.54 Å, and the angles (Ni-Te-Ni) and (Te-Ni-Te) are equal at 89.933°, while the angle

(Te-Ni-Te'), of which Te and Te' belong to two different groups, is 70.624° , taken from Ref. [9]. These parameters are used to build the pristine 1H-NiTe₂ structure.

Stillinger-Weber potential is adopted to simulate the interatomic interactions [9] in the present study. The potential energy E of the atomic structure is the sum of the bond stretching E_r and bond angle bending energy E_θ :

$$E = E_r + E_\theta, \quad (1)$$

$$E_r = \sum_{e=1}^M V_2, \quad E_\theta = \sum_{e=1}^N V_3, \quad (2)$$

$$V_2 = Ae^{\left[\frac{\rho}{r_{ij}-r_{\max ij}}\right]} \left(B/r_{ij}^4 - 1 \right), \quad (3)$$

$$V_3 = Ke^{\left[\frac{\rho_{ij}}{r_{ij}-r_{\max ij}} + \frac{\rho_{ik}}{r_{ik}-r_{\max ik}}\right]} \left(\cos \theta_{ijk} - \cos \theta_0 \right)^2, \quad (4)$$

where V_2 corresponds to the bond-stretching and V_3 to the angle-bending. M and N denote the total numbers of bond-stretching and angle-bending elements, respectively (Figure 2). The cutoffs $r_{\max ij}, r_{\max ik}$ are determined from the nanomaterial's structure. A, K are energy parameters. $\rho, B, \rho_{ij}, \rho_{ik}$ and θ_0 are five geometrical parameters. r_{ij}, r_{ik} are the length of bonds ij and ik , respectively. θ_{ijk} is the angle between two bonds ij and ik . They can be defined as below:

$$r_{ij} = \sqrt{(x_j - x_i)^2 + (y_j - y_i)^2 + (z_j - z_i)^2}, \quad (5)$$

$$\cos \theta_{ijk} = \frac{(x_j - x_i)(x_k - x_i) + (y_j - y_i)(y_k - y_i) + (z_j - z_i)(z_k - z_i)}{r_{ij} \cdot r_{ik}}, \quad (6)$$

here $(x_i, y_i, z_i), (x_j, y_j, z_j)$ and (x_k, y_k, z_k) are coordinates of atoms i, j and k , respectively.

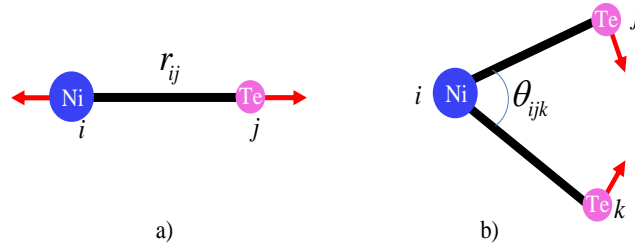


Figure 2. Two types of elements in SW potential: a) Bond-stretching element and b) Angle-bending element in the 1H-NiTe₂ structure.

Stillinger-Weber potential parameters are taken from Ref. [9] for 1H-NiTe₂ nanosheets and listed in Tables 1 and 2.

Table 1. Bond-stretching SW potential parameters of 1H-NiTe₂ sheet.

	A (eV)	ρ (Å)	B (Å ⁴)	$r_{\max ik}$ (Å)
Ni-Te	6.461	1.359	20.812	3.469

Molecular dynamic finite element method, which has successfully estimated the mechanical behaviors of some hexagonal sheets with Tersoff potentials in our previous works [12, 13], is here further developed for SW potential to research the mechanical behaviors of 1H-

NiTe₂ nanosheets. A more detailed procedure of MDFEM is introduced in our previous work [12].

Table 2. Angle-bending SW potential parameters of 1H-NiTe₂ sheet. Te-Ni-Te indicates the bending energy for the angle with Ni as the apex.

	K (eV)	θ_0 (degree)	ρ_{ij} (Å)	ρ_{ik} (Å)	r_{maxij} (Å)	r_{maxik} (Å)	r_{maxjk} (Å)
Te-Ni-Te	24.759	89.993	1.359	1.359	3.469	3.469	4.114
Ni-Te-Ni	24.759	89.993	1.359	1.359	3.469	3.469	4.114
Te-Ni-Te'	27.821	70.624	1.359	1.359	3.469	3.469	4.114

Simple tensile tests of 1H-NiTe₂ nanosheets along the ZZ and AM directions were conducted. Young's modulus and Poisson's ratio were calculated by a linear fitting of the stress-strain curve in the strain smaller than 0.01. In this study, we used 2D Young's modulus (Y_t) and 2D stress (σ_t) with t being thickness of the nanosheet, σ and ϵ denoting the engineering stress and engineering strain, respectively.

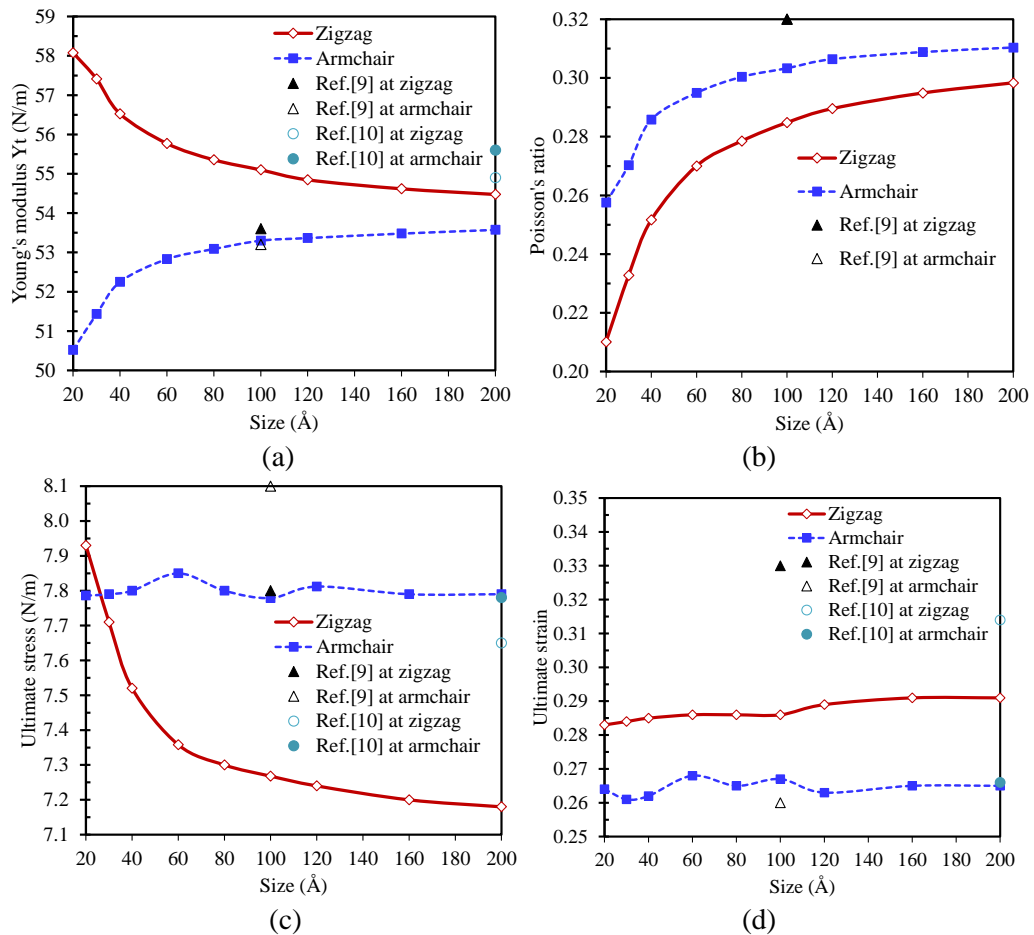


Figure 3. Influence of size of the square shaped 1H-NiTe₂ pristine sheets on (a) Young's modulus; (b) Poisson's ratio; (c) ultimate stress and (d) ultimate strain.

3. RESULTS AND DISCUSSION

To begin, square shaped 1H-NiTe₂ pristine nanosheets with dimensions between 20 × 20 Å and 200 × 200 Å are built to study size effects on their mechanical properties. Figure 3 shows data on the dependency of Young's modulus, Poisson's ratio, ultimate stress, and ultimate strain of the 1H-NiTe₂ pristine sheet on its size. The 2D Young's moduli are 58.1 N/m and 50.5 N/m along the ZZ and AM directions, respectively, in the smallest sheet, then decrease to 54.5 N/m along the ZZ direction but increase to 53.6 N/m along the AM one in the biggest sheet. These results are close to those by molecular dynamic simulations [9, 10]. In addition, the Young's modulus in both directions has tendency to reach the same value in bigger sheets which shows that the Young's modulus of the 1H-NiTe₂ nanosheet is isotropic in the ZZ and AM directions. Similar phenomenon has been reported for monolayer 1H-MoS₂ nanosheets [14, 15].

As shown in Figure 3b, the Poisson's ratios increase as the size gets larger. For the 200 Å square shaped sheet, the values are 0.30 and 0.31 in the ZZ and AM directions, respectively, which are close to the value of 0.32 by using molecular dynamic simulations [9]. The influence of the size of the nanosheet on the ultimate stress and ultimate strain is introduced in Figures 3c, 3d. When the size of the 1H-NiTe₂ nanosheet becomes bigger, from 20 to 200 Å, the ultimate stress in the ZZ direction shows a decrease from 7.9 N/m to 7.2 N/m, while that in the AM one is nearly unchanged at 7.8 N/m and ultimate strains in the AM direction slightly fluctuate around 26.4 %, and that in the ZZ one slightly increases from 28.3 % to 29.1 %.

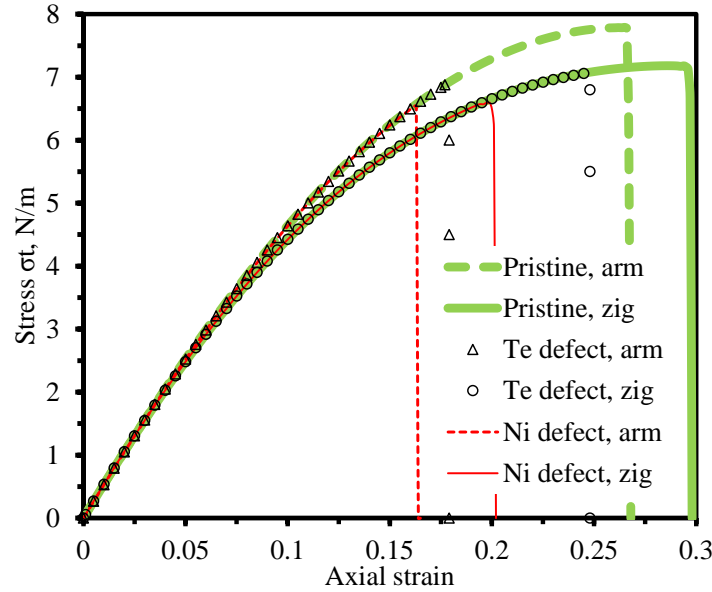


Figure 4. Stress-strain curves of 1H-NiTe₂ nanosheet with an atom vacancy defect in the sheet's center under simple tensile tests.

Next, the effect of vacancy defects on the mechanical properties of 1H-NiTe₂ nanosheet will be investigated. Vacancy defects are a type of point defect where an atom is missing. They occur naturally in all crystalline nanomaterials and 1H-NiTe₂ is no exception. Two cases of defects, missing a Ni atom and missing a Te atom at the 200 × 200 Å sheet's center, are considered in the present work. Stress-strain curves of the 1H-NiTe₂ defect sheet with different types of missing atom are drawn in Figure 4. The results show that the stress-strain curves of

defected nanosheets coincide with those of pristine sheets up to the corresponding fracture points. Therefore, the defected nanosheets possess nearly the same value of Young's modulus as the pristine one with that being around 54 N/m along both the ZZ and AM directions. A similar phenomenon can be seen in the Poisson's ratio. However, the defects have significant effects on ultimate stress and strain. With missing a Te atom in the sheet's center, the ultimate stress decreases from 7.2 N/m to 7.1 N/m and from 7.8 N/m to 6.9 along the ZZ and AM directions, respectively. In addition, the ultimate strain also undergoes a decrease from 29.1 % to 24.5 % in the ZZ direction and from 26.5 % to 17.7 % in the AM one. Besides, missing a Ni atom stronger affects the ultimate stress and ultimate strain with the former declining to 6.6 N/m (along the ZZ direction), 6.5 N/m (along the AM one), and the latter declining to 19.5 % (along the ZZ one), 16.3 % (along the AM one). The sheet is more weakened by missing a Ni atom than by missing a Te one due to Ni atoms located on the central layer with each Ni atom linking to six Te ones while a Te atom being on the surface layer is bonded to only three Ni ones (see Figure 1). Therefore, six bond-stretchings vanish with missing a Ni atom while only three ones disappear with missing a Te atom.

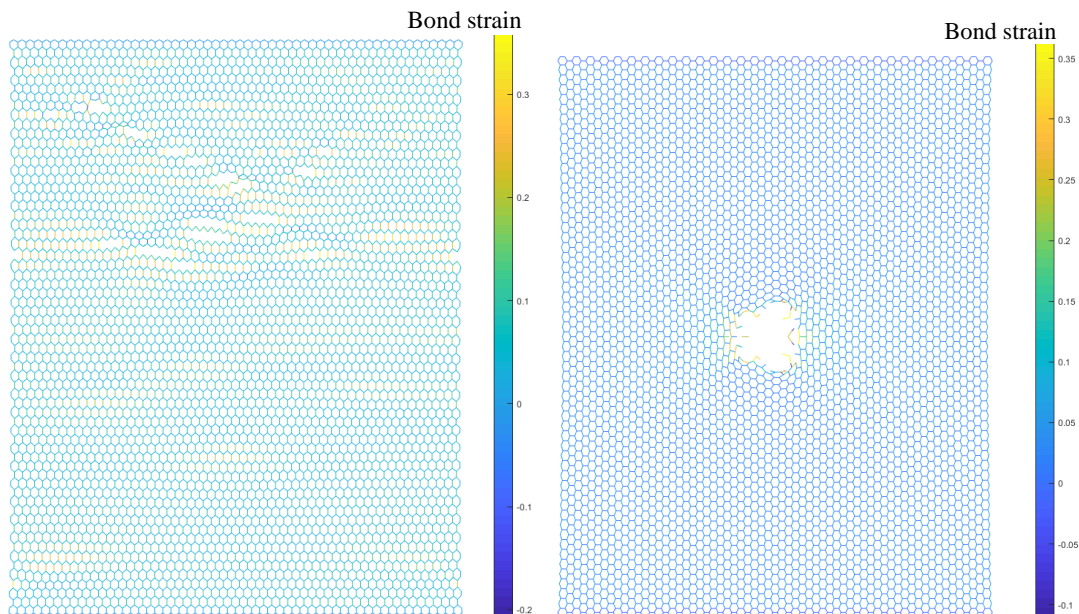


Figure 5. Photographs of 1H-NiTe₂ pristine (left) and vacancy defect (right) sheet at fracture point.

Figure 5 gives photographs of the fracture nanosheet under simple tensile tests, where a bond is not shown if its length exceeds the maximum value of 3.469 Å. It can be seen that the fracture occurs in a line perpendicular to the direction of the loading. However, the fracture is located in the sheet's center where the point defect is. Because the sheet is naturally weakened by missing atom, a hole becomes bigger and bigger from the defected location during the nanosheet's tension which leads to a failure at the defected location as shown in Figure 5.

4. CONCLUSIONS

To summarize, the mechanical properties of 1H-NiTe₂ pristine and defected sheets under uniaxial tension have been investigated using MDFEM with SW potential. With the pristine

sheet, the Young's modulus increases in the AM direction but decreases in the ZZ one when the dimension of the sheet becomes bigger, but they are nearly same value in the large sheet. In addition, ultimate stress in the AM direction remains nearly unchanged while that in the ZZ one significantly decreases when the size of the sheet gets larger. The Poisson's ratio goes up as the size gets bigger, but it has a slower rise in the larger sheets. Besides the size effect, vacancy defects are also studied. It is found that an atom missing defect strongly affects the ultimate stress and ultimate strain but has almost no effect on Young's modulus and Poisson's ratio of 1H-NiTe₂. Because of a point defect in the sheet's center, the ultimate stress and strain decline about 1.7 - 16.0 % and 15.8 - 38.5 %, respectively. Our findings in this work provide useful information for the design of nanodevices using 1H-NiTe₂ nanosheets in future applications.

Although various nanomaterials have been calculated by DFT calculations and MD simulations, such computational techniques are all time-consuming and high-performance computing requirements. Our approach of using MDFEM here is a simple and fast technique to accurately study the mechanical properties of 1H-NiTe₂ nanosheets. Until now, the limitation of the MDFEM is that it is only used to calculate the mechanical properties without temperature effect. We hope that MDFEM can be developed to study more aspects of nanomaterials in our future works.

CRedit authorship contribution statement. Nguyen Danh Truong: Data analysis, Writing–review and editing, Supervision. Nguyen Van Quynh: Modeling, Preparing data.

Declaration of competing interest. The authors declare that they have no known competing financial interests or personal relationships that could have appeared to influence the work reported in this paper.

REFERENCES

1. Singh S., Hasan M. R., Sharma P., Narang J. - Graphene nanomaterials: The wondering material from synthesis to applications, *Sensors International*, 2022, pp.100190. <https://doi.org/10.1016/j.sintl.2022.100190>.
2. Radisavljevic B., Radenovic A., Brivio J., Giacometti V., Kis A. - Single-layer MoS₂ transistors, *Nature Nanotechnology* **6** (2011) 147-150. <https://doi.org/10.1038/nnano.2010.279>.
3. Lopez-Sanchez O., Lembke D., Kayci M., Radenovic A., Kis A. - Ultrasensitive photodetectors based on monolayer MoS₂, *Nature Nanotechnology* **8** (2013) 497-501. <https://doi.org/10.1038/nnano.2013.100>.
4. Mak K. F., Lee C., Hone J., Shan J., Heinz T. F. - Atomically Thin MoS₂: A New Direct-Gap Semiconductor, *Physical Review Letters* **105** (2010) 136805. <https://doi.org/10.1103/PhysRevLett.105.136805>.
5. Huo N., Yang Y., Li J. - Optoelectronics based on 2D TMDs and heterostructures. *Journal of Semiconductors* **38** (2017) 031002. <https://doi.org/10.1088/1674-4926/38/3/031002>.
6. Chia X., Sofer Z., Luxa J., Pumera M. - Unconventionally Layered CoTe₂ and NiTe₂ as Electrocatalysts for Hydrogen Evolution, *Chemistry A European Journal*, **23** (2017) 11719-11726. <https://doi.org/10.1002/chem.201702753>.
7. Zhao B., Dang W., Liu Y., Li B., Li J., Luo J., Zhang Z., Wu R., Ma H., Sun G., Huang Y., Duan X., Duan X. - Synthetic Control of Two-Dimensional NiTe₂ Single Crystals

- with Highly Uniform Thickness Distributions, *Journal of the American Chemical Society* **140** (2018) 14217-14223. <https://doi.org/10.1021/jacs.8b08124>.
8. Nappini S., Boukhvalov D. W., D'Olimpio G., Zhang L., Ghosh B., Kuo C. N., Zhu H., Cheng J., Nardone M., Ottaviano L., Mondal D., Edla R., Fuji J., Lue C. S., Vobornik I., Yarmoff J. A., Agarwal A., Wang L., Zhang L., Bondino F., Politano A. - Transition-Metal Dichalcogenide NiTe₂: An Ambient-Stable Material for Catalysis and Nanoelectronics, *Advanced Functional Materials* **30** (2020) 2000915. <https://doi.org/10.1002/adfm.202000915>.
 9. Jiang J. W., Zhou Y. P. - Parameterization of Stillinger-Weber potential for two-dimensional atomic crystals, *ArXiv* (2017) 484. <https://doi.org/10.48550/arXiv.1704.03147>.
 10. Jamil M. F., Subad R. A. S. I., Akash T. S., Bose P. - Intrinsic mechanical properties of monolayer nickel ditelluride: An atomistic study, *Computational Condensed Matter* **26** (2021) e00522. <https://doi.org/10.1016/j.cocom.2020.e00522>.
 11. Ruzsinszky L. Y. a. Q. Y. A. A. - Negative Poisson's ratio in 1T-type crystalline two-dimensional transition metal dichalcogenides, *Nature Communications* **8** (2017) 1-8. <https://doi.org/10.1038/ncomms15224>.
 12. Le M.-Q., Nguyen D.-T. - Atomistic simulations of pristine and defective hexagonal BN and SiC sheets under uniaxial tension. *Materials Science and Engineering: A*, **615** (2014) 481-488. <https://doi.org/10.1016/j.msea.2014.07.109>.
 13. Nguyen D. T., Le M. Q., Nguyen V. T., Bui T. L. - Effects of various defects on the mechanical properties of black phosphorene, *Superlattices and Microstructures* **112** (2017) 186-199. <https://doi.org/10.1016/j.spmi.2017.09.021>.
 14. Bao H., Huang Y., Ma F., Yang Z., Miao Y., Xu K., Chu P. K. - Size-dependent elastic modulus of single-layer MoS₂ nano-sheets, *Journal of Materials Science* **51** (2016) 6850-6859. <https://doi.org/10.1007/s10853-016-9972-x>.
 15. Nguyen D. T. - Size Effects on Mechanical Properties of Single Layer Molybdenum Disulfide Nanoribbon, *Advances in Asian Mechanism and Machine Science*, Springer International Publishing, Vol. 113, Cham, 2022, pp. 705-715.